J. Membrane Biol. 175, 107–113 (2000)

The Journal of
Membrane
Biology

Effect of Ferriprotoporphyrin IX and Non-heme Iron on the Ca^{2+} Pump of Intact Human Red Cells

T. Tiffert, V.L. Lew, D. Perdomo, H. Ginsburg*
Physiological Laboratory, University of Cambridge, Downing Street, Cambridge CB2 3EG, United Kingdom

Received: 22 November 1999/Revised: 29 February 2000

Abstract. Previous studies have shown that ferriprotoporphyrin IX (FP) and non-heme iron have a marked inhibitory effect on the Ca^{2+}-Mg^{2+}-ATPase activity of isolated red cell membranes, the biochemical counterpart of the plasma membrane Ca^{2+} pump (PMCA). High levels of membrane-bound FP and non-heme iron have been found in abnormal red cells such as sickle cells and malaria-infected red cells, associated with a reduced life span. It was important to establish whether sublytic concentrations of FP and non-heme iron would also inhibit the PMCA in normal red cells, to assess the possible role of these agents in the altered Ca^{2+} homeostasis of abnormal cells. Active Ca^{2+} extrusion by the plasma membrane Ca^{2+} pump was measured in intact red cells that had been briefly preloaded with Ca^{2+} by means of the ionophore A23187. The FP and nonheme iron concentrations used in this study were within the range of those applied to the isolated red cell membrane preparations. The results showed that FP caused a marginal inhibition (~20%) of pump-mediated Ca^{2+} extrusion and that non-heme iron induced a slight stimulation of the Ca^{2+} efflux (11–20%), in contrast to the marked inhibitory effects on the Ca^{2+}-Mg^{2+}-ATPase of isolated membranes. Thus, FP and non-heme iron are unlikely to play a significant role in the altered Ca^{2+} homeostasis of abnormal red cells.

Key words: Ferriprotoporphyrin IX — Heme — Non-heme iron — Ca^{2+}-pump — Red blood cells

* *Permanent address:* Department of Biological Chemistry, Institute of Life Sciences, The Hebrew University of Jerusalem, Jerusalem 91904, Israel

Correspondence to: T. Tiffert

Introduction

Methemoglobin and hemichromes bind to the inner face of the red cell membrane and release ferriprotoporphyrin IX (FP). FP is a highly lipophilic compound [3, 38] present mostly at the lipid-water interface of the membrane [15]. FP destabilizes the membrane structure [8, 40], increases the membrane ion permeability [9], induces lipid peroxidation [7], and stimulates protein crosslinking by oxydizing thiol groups [6, 23, 24, 48]. The erythrocyte membrane is normally protected from these effects by two major mechanisms: degradation of FP by cellular glutathione [1], and extraction of membrane-associated FP by albumin and hemopexin [43]. However, in certain pathological conditions associated with reduced red cell life span and hemolysis, such as in sickle cell anemia [27, 28], and in *Plasmodium falciparum*-infected red cells, particularly when chloroquine treated [50], high levels of red cell membrane-associated FP and non-heme iron have been detected. It is therefore important to investigate the effects of FP and non-heme iron on cell targets that might be critical to cell stability and survival.

Red cells are endowed with a powerful plasma membrane Ca^{2+} pump (PMCA) [4, 39] whose function has been claimed to be altered in vitro by both FP and non-heme iron. This could be of pathophysiological importance since the disturbed Ca^{2+} homeostasis of the cell may contribute to its early demise. The calmodulin-dependent Ca-Mg-ATPase activity of erythrocyte ghosts membranes, the biochemical expression of this pump, has been found to be inhibited by FP in a time- and concentration-dependent manner [30]. Similarly, non-heme iron, thought to be generated *in situ* from membrane-associated FP [27], has also been found to be an effective inhibitor [29]. The PMCA is a highly regulated pump [5, 20, 47]. Hence, it is uncertain whether the behavior of the Ca-Mg-ATPase in ghost membranes

preparations may be extrapolated to the function of the PMCA in the intact cell. The purpose of the experiments presented here was to investigate whether the PMCA function is affected by FP and by non-heme iron, in intact human red cells.

Ca^{2+} pump function in intact red cells is best assessed by measuring active Ca^{2+} extrusion from the cells. Since red cells are essentially Ca^{2+}-free [2, 13, 22], it is necessary to load them with Ca^{2+} first. This is achieved by means of divalent cation ionophores in Ca^{2+}-containing media. After Ca^{2+} loading, Ca^{2+} pump function is measured by stopping the passive Ca^{2+} fluxes through the ionophore, thereby exposing Ca^{2+} efflux through the pump [13, 34, 35, 42, 44]. The available methods were combined with specially designed protocols to provide the first direct measurements of the effects of FP and non-heme iron on PMCA function in the intact cell. The results obtained are at variance with those previously reported for Ca^{2+}-Mg^{2+}-ATPase activity in red cell membranes.

Materials and Methods

Solutions

Solution A contained (in mM): KCl, 80; NaCl, 70; $MgCl_2$, 0.15; HEPES-Na (pH 7.4–7.5 at 37°C), 10, and Na-EGTA, 0.1. Solution B was the same as solution A, but without Na-EGTA. Solution C was the same as solution B but contained, in addition, 10 mM inosine and 5 mM glucose. A stock solution of $^{45}CaCl_2$ was prepared at a concentration of 40 mM and with $^{45}Ca^{2+}$ specific activity of about 10^7 cpm $(\mu mol)^{-1}$. A23187 was dissolved in ethanol, as a 2 mM stock solution. $CoCl_2$ stock solutions were prepared in distilled water at concentrations between 70–100 mM. FP was prepared as a stock solution in 0.1 N NaOH immediately before use and kept on ice protected from light; this solution was diluted with the appropriate incubation medium before addition to cell suspensions to the final desired concentration. Chloroquine stock solutions were prepared in distilled water.

Preparation of RBCs

Venous blood from healthy volunteers was drawn into heparinized syringes, after written consent. The cells were washed 4 times by centrifugation (2,500 × *g*, 5 min) and resuspension in 5–10 volumes of medium; after each spin, the supernatant and the top cell layer containing white cells and platelets were removed. The first 2 washes were in solution A, to remove calcium loosely bound to the cells; the last 2 washes were in solution B, to remove EGTA from the medium. After the washes, the cells were suspended at about 10% hematocrit (Hct) in solution C, with or without additives, as indicated. These high-K media ensure the constancy of the physiological intracellular milieu and prevent those changes in RBC volume, pH and ion content (other than Ca^{2+}), that would occur after exposure of the cells to divalent cation ionophores in plasmalike, Ca^{2+}-containing media [16, 18, 31, 32]. The Hct in all cell suspensions was estimated from spectrophotometric measurements of hemoglobin (Hb) by the cyanmethemoglobin method.

Effects of FP on RBC Morphology and Hemolysis

The cell membrane destabilizing effects of FP are time- and concentration-dependent, causing changes in RBC shape and volume as well as hemolysis [8, 9]. Therefore, it was important to carry out a preliminary investigation of these effects, to assess the overall condition of the cells during Ca^{2+} flux measurements, and to establish the maximal FP concentration at which Ca^{2+} pump function could be tested without an undesirable degree of hemolysis. The effects of FP on red cell shape were observed in fresh, unfixed samples of RBC suspensions, under phase contrast at ×1,000. The samples were placed between glass slide and coverslip, observed, and videorecorded for leisured analysis at the end of experiments. The changes induced by FP on hemolysis curves, as a function of concentration and time, were assessed by the profile migration method [36, 37]. Hemolysis due to FP, and percent hemolysis, were estimated from spectrophotometric Hb measurements at 415 nm (Soret band), as previously described [33].

Measurements of PMCA-Mediated Ca^{2+} Extrusion

Preliminary experiments indicated that the simultaneous presence of FP and ionophore A23187 in cell suspensions caused extensive hemolysis, incompatible with Ca^{2+} pump function measurements. To avoid this problem, two different experimental protocols were designed. In the first protocol, designed to test the effects of FP on PMCA-mediated Ca^{2+} extrusion, Ca^{2+} pump function was measured in RBCs preloaded with $^{45}Ca^{2+}$ by means of ionophore, but from which the ionophore was removed with albumin prior to the measurements. In the second protocol, designed to study the effects of non-heme iron on PMCA-mediated Ca^{2+} extrusion, Ca^{2+} pump function was measured in RBCs by the Co^{2+}-exposure method [11]. Accumulation of non-heme iron in the cells was induced by pre-incubation with FP ± chloroquine, followed by removal of residual FP and chloroquine prior to pump-function measurement by the Co^{2+}-exposure method. Previous studies [1] have demonstrated that incubation of FP-loaded intact RBCs results in a time-dependent FP degradation. Most of the released iron remains associated with the membrane, while the dissociated iron is engaged in redox cycling producing oxidative radicals. Hence, this condition effectively reproduces that of non-heme iron and oxidative stress on the pump. Chloroquine was added in order to inhibit the degradation of FP [15]; this condition served as a control for possible effects of FP, other than those through non-heme iron production. As demonstrated before [35], the methods used here to measure Ca^{2+} pump function, i.e., after ionophore removal (first protocol), and after Co^{2+}-exposure (second protocol), provide comparable results in normal intact red cells. The protocols are described in detail next.

First Protocol: Effect of FP on PMCA-Mediated Ca^{2+} Extrusion

Washed RBCs were suspended at 10% Hct in solution C, and pre-incubated at 37°C for ~5 min to allow for equilibration while mixing continuously with a magnetic stirrer. $^{45}CaCl_2$ was then added to a final total calcium concentration ($[Ca_T]_s$) of 130 μM. Pre-incubation was continued for ≈10 min before adding ionophore A23187 to a final concentration of 10 μM in the suspension (~100 μmol (l cells)$^{-1}$). This ensured rapid $^{45}Ca^{2+}$ equilibration across the RBC membrane. Two min after A23187 addition, the ionophore was extracted by transferring the suspension to a tube containing twenty volumes of ice-cold solution A with 1.5% (w/v) fatty acid-free bovine serum albumin [42] and mixed. The cells were washed four times in this solution and packed (~80% Hct). For the final incubation, the packed cells were

delivered, under magnetic stirring, into prewarmed solution C, with either no additives or with 25 μM FP, to obtain a 10% Hct RBC suspension at ~37°C. Ca^{2+} extrusion under these conditions has been shown to be inhibited by ATP depletion and vanadate [11, 35, 45], and, therefore, to be PMCA-mediated. Once the incubation was started, suspension samples [50 μl] were taken at indicated times for measurements of total intracellular calcium $[Ca_T]_i$, as previously described [32]. The ionophore-induced Ca^{2+} uptake and PMCA-mediated Ca^{2+} extrusion rates were estimated from plots of $[Ca_{Ti}]$ *vs.* time.

Second Protocol: Effect of Non-heme Iron on PMCA-Mediated Ca^{2+} Extrusion

Washed RBCs were suspended at 10% Hct in solution C, without or with any of the following additives: 25 μM FP, 10 μM chloroquine, or 10 μM FP + 10 μM chloroquine, and pre-incubated at 37°C for 1 hr under continuous stirring. Chloroquine prevents FP degradation and non-heme iron production [21], but co-incubation of chloroquine and FP enhances hemolysis [10, 12]. Therefore, the concentrations chosen for combined use of these compounds were the highest compatible with less than 10% hemolysis, in blood from the 4 donors investigated, during 60–80 min pre-incubation at 37°C (*data not shown*). Following pre-incubation with FP, the cells were washed twice in solution B with 1% (w/v) fatty acid-free bovine serum albumin to remove all nondegraded FP, twice more in solution B without albumin, and packed. The cells were then resuspended at 10% Hct, 37°C, in solution C, for uphill Ca^{2+} extrusion measurements by the Co^{2+}-exposure method [11]. Briefly, after ~5 min equilibration under continuous stirring, $^{45}CaCl_2$ was added to a final ($[Ca_T]_s$) of 130 μM. The suspension was further pre-incubated for ~10 min before adding ionophore A23187, from a 2 mM stock solution, to a final concentration of 10 μM in the suspension (~100 μmol (l cells)$^{-1}$). This concentration allowed rapid $^{45}Ca^{2+}$ equilibration across the cell membrane. Two min later, $CoCl_2$ was added to a final concentration of ~250 μM in the suspension, sufficient to block all ionophore-mediated Ca^{2+} transport, and to expose the uphill extrusion of Ca^{2+} by the PMCA. Samples (50 μl) were taken throughout the procedure for determination of $[Ca_T]_i$, as described above.

Materials

Ferriprotoporphyrin IX chloride (FP) was from Porphyrin Products, Logan, Utah. Chloroquine, orthovanadate, EGTA, DMSO, HEPES, inosine, glucose, $CoCl_2$, and bovine albumin were from Sigma Chemical (UK). A23187 was from Calbiochem-Novabiochem (UK) Ltd. $CaCl_2$, $MgCl_2$, NaCl, and KCl were from FSA Laboratory Supplies (UK). $^{45}Ca^{2+}$ was from Amersham International plc (UK).

Abbreviations

FP, ferriprotoporphyrin IX; PMCA, plasma membrane Ca^{2+} pump; $[Ca_T]_s$, total calcium concentration in suspension; $[Ca_T]_i$, total intracellular calcium.

Results

Changes in Cell Morphology, Osmotic Fragility, and Hemolysis by FP

The changes in shape, osmotic fragility and hemolysis, induced by FP, were found to be dependent on FP concentration, temperature, time, external Ca^{2+} concentration, presence of ionophore A23187, and donor. We briefly report here only the features relevant to the condition of the cells used for Ca^{2+} transport studies.

Addition of FP to an RBC suspension caused an immediate cell shape transformation. From biconcave disks, the cells transformed, at progressively increasing FP concentrations, to sharply spiculated echinocytes ([FP] $\leq$ 10 μM), and spherocytes (FP > 10–20 μM, depending on the suspension Hct) with their surface ruffled by very fine microvilli. Our optical microscopy on fresh, unfixed samples, were in full agreement with those documented before by scanning electron microscopy on fixed specimens [8]. The spherocytic appearance of RBCs at high FP concentrations was reminiscent of that induced by detergents used in cell sorting procedures [25], suggesting that the mechanism of the cell shape changes by FP may be similar. Removal of FP with albumin restored the biconcave shape immediately, demonstrating the reversibility of this effect, and confirming the efficiency of the albumin extraction procedure. To investigate the effect of intracellular FP degradation on cell morphology we followed in time the spontaneous shape changes of cells suspended at 10% Hct, 37°C, in solution C with 25 μM FP. Starting with a uniform population of spherocytes, the cells slowly reversed back to biconcave disks, recapitulating the intermediate spiculated echynocytic forms documented at lower FP concentrations. The first biconcave disk forms appeared at about four hours; by 12–18 hr all unlysed cells had regained their original biconcave shape. These results indicated that the FP concentration was gradually decreasing, as would be expected from the erythrocyte ability to degrade FP.

Figure 1 shows the time-dependent effects of FP, with and without Ca^{2+}, on RBC osmotic fragility. Addition of 20 μM FP to a red cell suspension (10% Hct) at 37°C, caused an immediate right-shift in the hemolysis curves indicative of a sudden increase in osmotic fragility, and coincident with the shape changes described above. FP elicited two additional time-dependent effects, with a slow time course. The first effect was a gradual increase in the fraction of hemolyzed cells, indicated by the progressive elevation of the baseline between 0.7 and 1.2 relative tonicity values (Fig. 1, both panels). Note that this is not osmotic lysis because the fraction of lysed cells remains invariant with tonicity, even at the slightly hypertonic condition included here. The detergentlike effect of FP on cell morphology described above may also be responsible for the observed nonosmotic lysis of a sensitive subpopulation of cells. The second effect concerns the time-dependent changes in osmotic fragility. The maximal increase in osmotic fragility, as indicated by the right-shift of the hemolysis curves, is observed at 1 min (Fig. 1, lower panel). Thereafter, the hemolysis curves shift back to the left towards

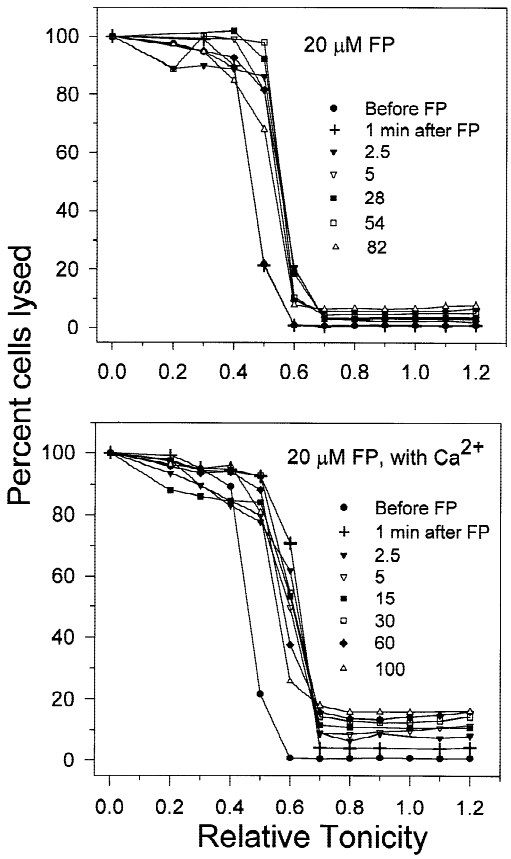

Fig. 1. Effect of FP and Ca^{2+} on the osmotic fragility of normal human red cells as a function of time. The hemolysis curves were obtained by the profile migration method of Lew et al. [33]. The cells were suspended at 3% Hct in solutions A (*top panel*) or solution B with 130 μM Ca^{2+} (*bottom panel*), both supplemented with 5 mM ionosine, and incubated at 37°C. At time = 0, FP was added to the cell suspension to a final concentration of 20 μM. Samples for hemolysis curves were taken at the indicated times. Relative tonicities above 1 were obtained by addition of sucrose, 30 and 60 mM for 1.1 and 1.2, respectively. High tonicities were explored to establish whether or not the progressive hemolysis observed at relative tonicities above 0.7 was due to increased osmotic fragility. The low relative tonicities were obtained by dilution of solutions A or B with a solution containing 1 mM of HEPES-Na (pH 7.5).

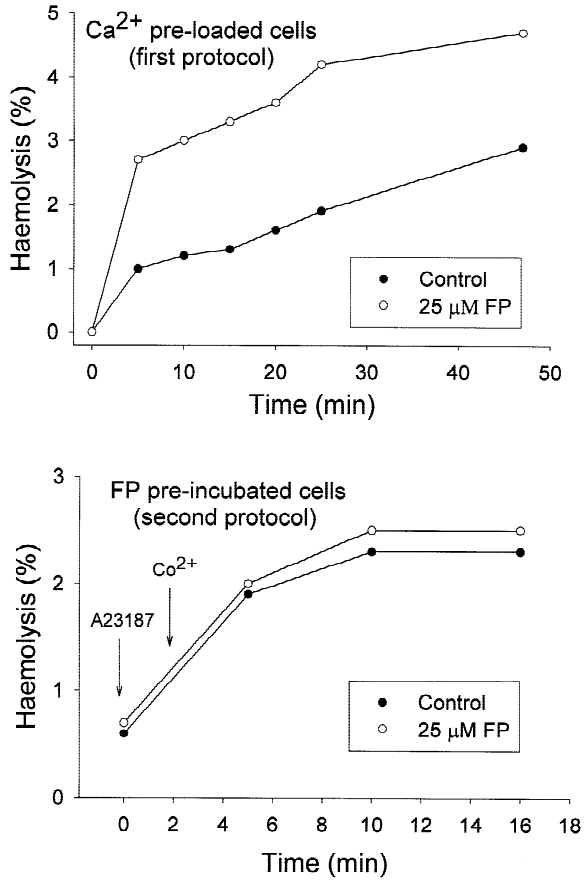

Fig. 2. Combined hemolysis effects of red cell exposure to ionophore A23187 and FP in the conditions of the Ca^{2+}-extrusion measurements (protocols 1 and 2). *Upper panel:* hemolysis in suspension of Ca^{2+} preloaded cells (10% Hct, 37°C) in the absence (filled circles, controls) and presence (unfilled circles) of FP. At time = 0, the Ca^{2+} preloaded RBCs were delivered into solution C with or without 25 μM FP. *Lower panel:* hemolysis in suspension of RBCs pre-incubated with (unfilled circles) or without (filled circles) FP and processed by the Co^{2+}-exposure protocol. The cells were pre-incubated with or without 25 μM FP for 80 min at 37°C. Hemolysis during pre-incubation with FP was ~6–8%. After the pre-incubation, nondegraded FP was removed and the cells were resuspended in solution C (10% Hct, 37°C) with 130 μM $^{45}Ca^{2+}$. Ionophore A23187 was added to 10 μM at time = 0, followed by Co^{2+} addition at 2 min. Hb was measured in the supernatant of samples taken at the indicated times.

that of FP-free controls. The shift is not uniform, as reflected by the shallower profile of the intermediate time curves suggesting that progressively more cells tend to regain the lower osmotic fragility status of the controls. This is consistent with reversibility of the FP effects as a result of its progressive degradation. The magnitude of the effects on osmotic fragility and hemolysis increased with FP concentration (*not shown*), co-incubation of FP with Ca^{2+} (compare top and bottom panels in Fig. 1), and Ca^{2+} concentration (*not shown*). Although the FP effects were qualitatively similar among the RBCs from the 4 normal donors, the concentration-dependence varied considerably. Also the hemolytic effects of FP varied among donors and were not linear with concentration. At concentrations of FP in excess of 30 μM, hemolysis reached up to 40% in Ca^{2+}-containing media. 25 μM was the maximal concentration compatible with an acceptable level of hemolysis (3% or less) and was therefore chosen for the Ca^{2+} flux measurements reported here.

Figure 2 reports the time-dependent hemolysis detected in conditions identical to those of the two experimental protocols used for PMCA-mediated Ca^{2+} extrusion measurements. Hemolysis was followed for incubation times in excess of the 8 min required for such

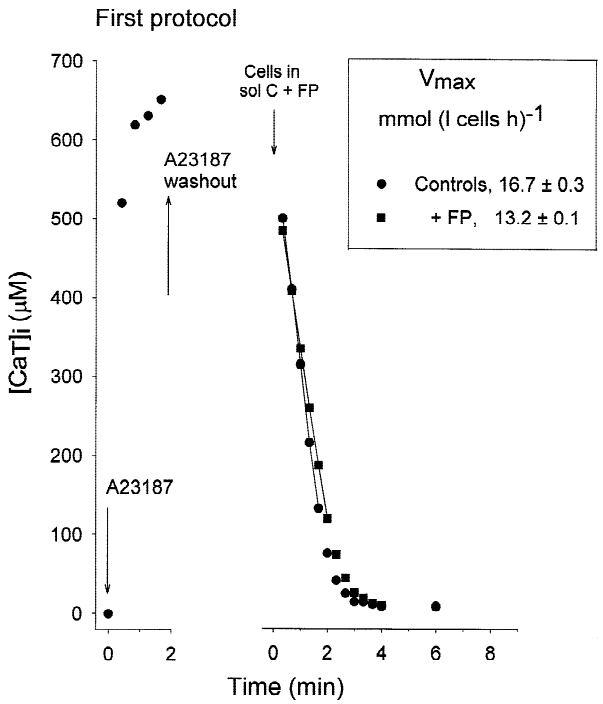

Fig. 3. Effect of FP on PMCA-mediated Ca^{2+} efflux. Ca^{2+} preloaded cells (first protocol) were suspended in solution C, without (circles, controls) and with (squares) 25 μM FP. $[Ca_T]_i$ is plotted as a function of time. The regression lines through the selected points represent the V_{max} of the Ca^{2+} pump. Pump V_{max} is reported as the mean ± SE of the slope, in mmol (l cells hr)$^{-1}$.

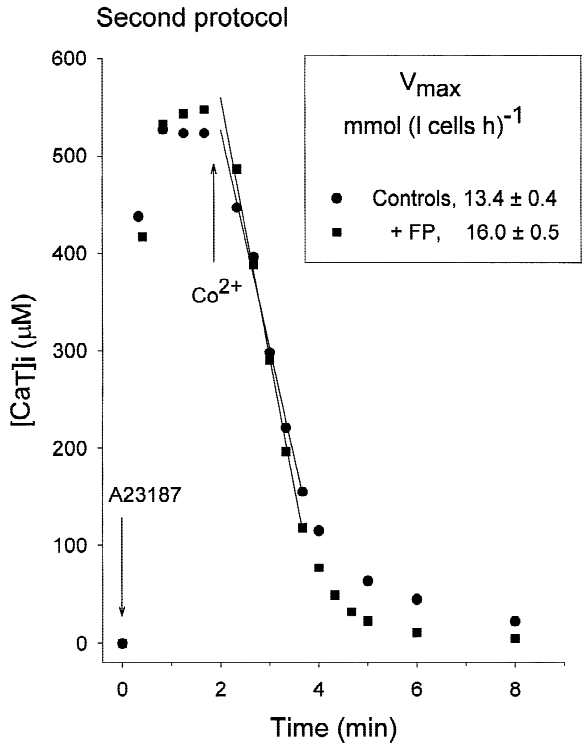

Fig. 4. Effect of non-heme iron on PMCA-mediated Ca^{2+} efflux. RBCs were pre-incubated for 1 hr at 37°C with (squares) and without (circles, controls) 25 μM FP. Nondegraded FP was then washed out with albumin before the cells were resuspended in solution C for measurement of PMCA-mediated Ca^{2+} extrusion by the Co^{2+}-exposure method. Pump V_{max} is reported as the mean ± SE of the slope, in mmol (l cells hr)$^{-1}$.

measurements (*see below*). The results show that hemolysis by FP never exceeded 3% throughout the period of Ca^{2+} flux measurements in all conditions.

Effects of FP and Non-Heme Iron on PMCA-Mediated Ca^{2+} Efflux

The effects of FP and non-heme iron on PMCA-mediated Ca^{2+} efflux are illustrated in Figs. 3 and 4, respectively. Vanadate (1 mM) fully inhibited Ca^{2+} efflux in all conditions (*not shown*), confirming that the efflux represented pump-mediated Ca^{2+} extrusion. In the experiment of Fig. 3 the cells were preloaded with Ca^{2+} to a $[Ca_T]_i$ level of about 670 μmol (1 cells)$^{-1}$. After ionophore removal (first protocol) the $[Ca_T]_i$ load was almost fully extruded within 3 min both in the absence (controls) and presence of FP. The function of the pump is thus largely conserved in the presence of FP.

The relation between total Ca^{2+} content and ionized Ca^{2+} concentration ($[Ca^{2+}]_i$) in normal red cells is well approximated by the relation $[Ca^{2+}]_i \sim \alpha[Ca_T]_i$, where $\alpha \sim 0.3$ over a wide range of $[Ca_T]_i$ values spanning those reported here [17, 46]. Down to a $[Ca_T]_i$ of about 100 μmol (l cells)$^{-1}$ the $[Ca^{2+}]_i$ level within the cells would have exceeded 30 μM, far above the submicromolar Ca^{2+} dissociation constant of the pump [20, 26]. Therefore, the initial Ca^{2+} efflux (Fig. 3), linear for at least 90 sec, represents the maximal Ca^{2+} extrusion rate by a $[Ca^{2+}]_i$-saturated pump (V_{max}). In this experiment, the V_{max} was inhibited by about 21% relative to controls. In a second similar experiment, 25 μM FP reduced the V_{max} by 23%, from 12.8 ± 0.2 in the controls, to 9.8 ± 0.2 mmol (l cells hr)$^{-1}$.

The effects of non-heme iron on pump-mediated Ca^{2+} extrusion are illustrated in Fig 4. Nearly complete uphill extrusion of the initial $[Ca_T]_i$ load of ~550 μmol (l cells)$^{-1}$ was accomplished within 3 min in test and control conditions, indicating full conservation of pump function. The V_{max} of the pump in the cells pre-incubated with 25 μM FP was increased by about 20% relative to both controls and to cells pretreated with FP and chloroquine (*not shown*). An increase of 11% (from 15.7 ± 0.3 to 17.4 ± 0.2 mmol (l cells hr)$^{-1}$) was observed in a second identical experiment. The V_{max} values obtained from cells pre-incubated in the presence of chloroquine (±FP) were not significantly different from controls (controls: 12.8 ± 0.2; 10 μM chloroquine: 12.2 ±

0.3; and 10 μM each chloroquine and FP: 13.4 ± 0.4 mmol (l cells hr)$^{-1}$).

Discussion

The results presented here showed that the function of the Ca^{2+} pump is largely preserved in intact red cells treated with FP or non-heme iron. This is in marked contrast with the powerful inhibitory effects reported earlier for similar FP or non-heme iron concentrations on the Ca^{2+}-Mg^{2+}-ATPase activity of ghost membranes [29, 30, 49], and stresses the difficulties of extrapolating results from biochemical tests on membrane fragments to functional tests in intact cells.

For a pump with the large spare capacity of the red cell PMCA, the 20–25% inhibition observed here at maximal sublytic FP concentrations is hardly significant in normal RBCs because of their low Ca^{2+} permeability. However, in cells with increased Ca^{2+} permeability, this minor pump deficit may contribute to elevate $[Ca^{2+}]_i$ to critical levels for certain intracellular Ca^{2+} targets, a consideration of potential relevance to the mechanism of sickle cell dehydration [14] or to the homeostasis of *P. falciparum*-infected red cells [41].

The high levels of FP used here are probably never met in vivo for two reasons: first, the rate of FP release from oxidized hemoglobin is easily matched by the rate of its degradation by glutathione at the inner membrane surface [1]; second, FP partitions rapidly between the two phospholipid monolayers and is rapidly extracted from the outer layer by serum hemopexin and albumin [3, 38, 43]. This also explains our observations of rapid and complete reversibility of the FP-induced shape transformations by albumin washes.

Whereas the degradation of FP by glutathione protects the cell from the toxic effects of FP, it also leaves a considerable amount of iron associated with the membrane. The redox-cycling of this iron causes lipid peroxidation and oxidation of essential protein SH groups. This condition was simulated here by pre-incubating the cells with high concentrations of exogenous FP prior to testing Ca^{2+} pump activity. During the pre-incubation of red cells with FP, much of the porphyrin was expected to be degraded by glutathione; any undegraded FP was removed by albumin washes prior to the measurements of Ca^{2+} pump function. With a $T_{1/2}$ of about 70 min for FP degradation, approximately 75% of non-heme iron would have become associated with the membrane [1]. At the end of the incubation the membrane fraction would have contained an amount of iron equivalent to ca. 100 μmol iron (10^{13} cells)$^{-1}$, well within the concentration range used by Leclerc et al. [29] to test the effect of iron on the ATPase activity of isolated membranes. These values compare to the levels of 34 nmol (mg protein)$^{-1}$ found in sickle ghosts [27] when using conversion factors of 3–4 g of membrane protein per 10^{13} ghosts. These iron levels are associated with increased levels of thiobarbituric acid reactive substances attesting the presence of lipid peroxidation. The ~20% inhibition of Ca^{2+}-Mg^{2+}-ATPase activity observed in ghost membranes at similar iron concentrations [29] contrasts with the slight enhancement (11–20%; Fig. 4) of pump activity documented here in the intact cell. This suggests that in the intact cell there are mechanisms at work that protect the membrane or the Ca^{2+} pump protein against iron injury, mechanisms absent in isolated membrane preparations. However, alternative explanations for the mild pump-stimulatory effects of iron cannot be ruled out. Hemolysis during the pre-incubation with FP was about 6–8%. It is conceivable that apparent stimulation may have resulted from the selective removal by lysis of subpopulations of low-pumping cells [19]. Whatever the reason for the differential effects obtained in isolated membranes and intact cells, the present observations stress the perils of extrapolating results in fragmented cells to the intact cell.

The authors thank The Wellcome Trust, and the Department of Physiology in Cambridge, for funds.

References

1. Atamna, H., Ginsburg, H. 1995. Heme degradation in the presence of glutathione. A proposed mechanism to account for the high levels of non-heme iron found in the membranes of hemoglobinopathic red blood cells. *J. Biol. Chem.* **270:**24876–24883
2. Bookchin, R.M., Lew, V.L. 1980. Progressive inhibition of the Ca pump and Ca:Ca exchange in sickle red cells. *Nature* **284:**561–563
3. Cannon, J.B., Kuo, F.-S., Pasternack, R.F., Wong, N.M., Muller-Eberhard, U. 1984. Kinetics of the interaction of hemin liposomes with heme binding proteins. *Biochemistry* **23:**3715–3721
4. Carafoli, E. 1992. The Ca^{2+} pump of the plasma membrane. *J. Biol. Chem.* **267:**2115–2118
5. Carafoli, E. 1997. Plasma membrane calcium pump: structure, function and relationships. *Basic Res. Cardiol.* **92 Suppl 1:**59–61
6. Chiu, D., Lubin, B. 1989. Oxidative hemoglobin denaturation and RBC destruction: the effect of heme on red cell membranes. *Semin. Hematol.* **26:**128–135
7. Chiu, D.T.-Y., van den Berg, J., Kuypers, F.A., Hung, I-J., Wei, J-S., Liu, T-Z. 1996. Correlation of membrane lipid peroxidation with oxidation of hemoglobin variants: possibly related to the rates of hemin release. *Free Radic. Biol. Med.* **21:**89–95
8. Chiu, D.T.-Y., Huang, T.-Y., Hung, I.-J., Wei, J.-S., Liu, T.-X., Stern, A. 1997. Hemin-induced membrane sulfhydryl oxidation: possible involvement of thiyl radicals. *Free Rad. Res.* **27:**55–62
9. Chou, A.C., Fitch, C.D. 1981. Mechanism of hemolysis induced by ferriprotoporphyrin IX. *J. Clin. Invest.* **68:**672–677
10. Chou, A.C., Fitch, C.D. 1993. Control of heme polymerase by chloroquine and other quinoline derivatives. *Biochem. Biophys. Res. Commun.* **195:**422–427
11. Dagher, G., Lew, V.L. 1988. Maximal calcium extrusion capacity and stoichiometry of the human red cell calcium pump. *J. Physiol.* **407:**569–586
12. Dutta, P., Fitch, C.D. 1983. Diverse membrane-active agents

modify the hemolytic response to ferriprotoporphyrin IX. *J. Pharmacol. Exp. Ther.* **225:**729–734
13. Engelmann, B., Duhm, J. 1987. Intracellular calcium content of human erythrocytes: relation to sodium transport systems. *J. Membrane Biol.* **98:**79–87
14. Etzion, Z., Tiffert, T., Bookchin, R.M., Lew, V.L. 1993. Effects of deoxygenation on active and passive Ca^{2+} transport and on the cytoplasmic Ca^{2+} levels of sickle cell anemia red cells. *J. Clin. Invest.* **92:**2489–2498
15. Famin, O., Krugliak, M., Ginsburg, H. 1999. Kinetics of inhibition of glutathione-mediated degradation of ferriprotoporphyrin IX by antimalarial drugs. *Biochem. Pharmacol.* **58:**59–68 (*in press*)
16. Ferreira, H.G., Lew, V.L. 1976. Use of ionophore A23187 to measure cytoplasmic Ca buffering and activation of the Ca pump by internal Ca. *Nature* **259:**47–49
17. Ferreira, H.G., Lew, V.L. 1977. Passive Ca transport and cytoplasmic Ca buffering in intact red cells. *In:* Membrane Transport in Red Cells. J.C. Ellory and V.L. Lew, editors. pp. 53–91. Academic Press, London
18. Freeman, C.J., Bookchin, R.M., Ortiz, O.E., Lew, V.L. 1987. K-permeabilized human red cells lose an alkaline, hypertonic fluid containing excess K over diffusible anions. *J. Membrane Biol.* **96:**235–241
19. García-Sancho, J., Lew, V.L. 1988. Heterogeneous calcium and adenosine triphosphate distribution in calcium-permeabilized human red cells. *J. Physiol.* **407:**523–539
20. Garrahan, P.J., Rega, A.F. 1986. The Ca^{2+} pump of plasma membranes. CRC Press, Boca Raton
21. Ginsburg, H., Famin, O., Zhang, J., Krugliak, M. 1998. Inhibition of glutathione-dependent degradation of heme by chloroquine and amodiaquine as a possible basis for their antimalarial mode of action. *Biochem. Pharmacol.* **56:**1305–1313
22. Harrison, D.G., Long, C. 1968. The calcium content of human erythrocytes. *J. Physiol.* **199:**367–381
23. Hebbel, R.P. 1990. The sickle erythrocyte in double jeopardy: auto-oxidation and iron decompartmentalization. *Semin. Hematol.* **27:**51–69
24. Hebbel, R.P., Eaton, J.W. 1989. Pathobiology of heme interaction with the erythrocyte membrane. *Semin. Hematol.* **26:**136–149
25. Kim, Y.R., Ornstein, L. 1983. Isovolumetric sphering of erythrocytes for more accurate and precise cell volume measurements by flow cytometry. *Cytometry* **3:**419–427
26. Kosk-Kosicka, D., Bzdega, T., Wawrzynow, A., Scaillet, S., Nemcek, K., Johnson, J.D. 1990. Erythrocyte Ca^{2+}-ATPase: activation by enzyme oligomerization versus by calmodulin. *In:* Calcium Binding Proteins in Normal and Transformed Cells. R. Pochet, E.M. Lawson and C.W. Heizmann, editors. pp. 169–174. Plenum Publishing
27. Kuross, A., Hebbel, R.P. 1988. Nonheme iron in sickle erythrocyte membranes: association with phospholipids and potential role in lipid peroxidation. *Blood* **72:**1278–1285
28. Kuross, S.A., Rank, B.H., Hebbel, R.P. 1988. Excess heme in sickle erythrocyte inside-out membranes: possible role in thiol oxidation. *Blood* **71:**876–882
29. Leclerc, L., Marden, M., Poyart, C. 1991. Inhibition of the erythrocyte (Ca^{2+} + Mg^{2+})-ATPase by nonheme iron. *Biochim. Biophys. Acta* **1062:**35–38
30. Leclerc, L., Vasseur, C., Bursaux, E., Marden, M., Poyart, C. 1988. Inhibition of membrane erythrocyte (Ca^{2+} + Mg^{2+})-ATPase by hemin. *Biochim. Biophys. Acta* **946:**49–56
31. Lew, V.L., Bookchin, R.M. 1986. Volume, pH and ion-content regulation in human red cells: analysis of transient behavior with an integrated model. *J. Membrane Biol.* **92:**57–74
32. Lew, V.L., García-Sancho, J. 1989. Measurement and control of intracellular calcium in intact red cells. *Methods Enzymol.* **173:**100–102
33. Lew, V.L., Raftos, J.E., Sorette, M.P., Bookchin, R.M., Monhandas, N. 1995. Generation of normal human red cell volume, hemoglobin content and membrane area distributions, by "birth" or regulation? *Blood* **86:**334–341
34. Lew, V.L., Simonsen, L.O. 1981. A23187-induced ^{45}Ca-flux kinetics reveals uniform ionophore distribution and cytoplasmic calcium buffering in ATP-depleted human red cells. *J. Physiol.* **316:**6P–7P
35. Pereira, A.C., Samellas, D., Tiffert, T., Lew, V.L. 1993. Inhibition of the calcium pump by high cystosolic Ca^{2+} in intact human red cells. *J. Physiol.* **461:**63–73
36. Raftos, J.E., Bookchin, R.M., Lew, V.L. 1996. Distribution of chloride permeabilities in normal human red cells. *J. Physiol.* **491:**773–777
37. Raftos, J.E., Bookchin, R.M., Lew, V.L. 1997. Measurement of the distribution of anion-exchange function in normal human red cells. *J. Physiol.* **499:**17–25
38. Rose, M.Y., Thompson, R.A., Light, W.R., Olson, J.S. 1985. Heme transfer between phospholipid membranes and uptake by apohemoglobin. *J. Biol. Chem.* **260:**6632–6640
39. Schatzmann, H.J. 1982. The plasma membrane calcium pump of erythrocytes and other animal cells. *In:* Membrane Transport of Calcium. E. Carafoli, editor. pp. 42–108. Academic Press, London
40. Schmitt, T.H., Frezzatti, W.A., Jr., Schreier, S. 1993. Hemin-induced lipid membrane disorder and increased permeability: a molecular model for the mechanism of cell lysis. *Arch. Biochem. Biophys.* **307:**96–103
41. Sherman, I.W. 1985. Membrane structure and function of malaria parasites and the infected erythrocyte. *PAR* **91:**609–645
42. Simonsen, L.O. 1981. Binding of ionophore A23187 by bovine plasma albumin. *J. Physiol.* **313:**34P–35P
43. Solar, I., Muller-Eberhard, U., Shaklai, N. 1989. Serum proteins as mediators of hemin efflux from red cell membranes: specificity of hemopexin. *FEBS Lett.* **256:**225–229
44. Tiffert, T., Etzion, Z., Bookchin, R.M., Lew, V.L. 1993. Effects of deoxygenation on active and passive Ca^{2+} transport and cytoplasmic Ca^{2+} buffering in normal human red cells. *J. Physiol.* **464:**529–544
45. Tiffert, T., Lew, V.L. 1997. Apparent Ca^{2+} dissociation constant of Ca^{2+} chelators incorporated non-disruptively into intact human red cells. *J. Physiol.* **505:**403–410
46. Tiffert, T., Lew, V.L. 1997. Cytoplasmic Ca^{2+} buffers in intact human red cells. *J. Physiol.* **500:**139–154
47. Wang, K.K.W, Villalobo, A., Roufogalis, B.D. 1992. The plasma membrane calcium pump: a multiregulated transporter. *Trends in Cell Biology* **2:**46–52
48. Winterbourn, C.C. 1990. Oxidative denaturation in congenital hemolytic anemias: the unstable hemoglobins. *Semin. Hematol.* **27:**41–50
49. Zaidi, A., Marden, M.C., Poyart, C., Leclerc, L. 1995. Protection by lazaroids of the erythrocyte (Ca^{2+}, Mg^{2+})-ATPase against iron-induced inhibition. *Eur. J. Pharmacol.* **290:**133–139
50. Zhang, J., Krugliak, M., Ginsburg, H. 1999. The fate of ferriprotoporphyrin IX in malaria infected erythrocytes in conjunction with the mode of action of antimalarial drugs. *Mol. Biochem. Parasitol.* **99:**129–141